Chemical Engineering Science 280 (2023) 119013

Contents lists available at ScienceDirect

Chemical Engineering Science

journal homepage: www.elsevier.com/locate/ces

Behavior of heavy metals and natural radionuclides along the Moroccan phosphogypsum carbonation process with several alkaline reagents

Brahim Bouargane [a], Silvia M. Pérez-Moreno [b], Alejandro Barba-Lobo [b,*], Bahcine Bakiz [c], Ali Atbir [a], Juan Pedro Bolívar [b]

[a] LGP, Faculty of Sciences, Ibn Zohr, University, B.P.: 8106, Agadir, Morocco
[b] Research Centre on Natural Resources, Health and Environment (RENSMA),Department of Integrated Sciences, University of Huelva, 21007 Huelva, Spain
[c] LME, Faculty of Sciences, Ibn Zohr University, B.P.: 8106, Agadir, Morocco

ARTICLE INFO

Keywords:
Phosphogypsum
Valorization
Mineral carbonation
Distribution
Trace elements
Radionuclides

ABSTRACT

Phosphogypsum (PG) is the main by-product from the phosphoric acid (PA) production industry being the PA production the basic raw material for producing the modern fertilizers. Because of its high calcium and sulfate content, it is important to emphasize that ecological benefits come from recycling and eventually converting PG into value-added compounds are obtained. This work aims to remedy the environmental problems associated to the large quantities of PG generated in Morocco. Furthermore, three procedures for PG conversion into $Ca(OH)_2$, $CaCO_3$, Na_2SO_4, K_2SO_4 and $(NH_4)_2SO_4$ using hydroxide aqueous mediums were studied. The impurity traces contained in the PG were generally found to be completely transferred into the final calcite. The sulfates produced here are recommended for the use as a fertilizer (K_2SO_4 and $(NH_4)_2SO_4$) and in the manufacture of detergents (Na_2SO_4), and the obtained calcite could be used in cement production, concretes, permeable reactive barriers for pollutants removing, etc.

1. Introduction

The phosphate industry and its derivatives have a remarkable income to the industry of Morocco (Bentaleb, 2019). It is of capital importance from both economic and social points of view to valorize their by-products to better address the market needs. Morocco is the worldwide leader of phosphate products and plays an important role in the global market. It is the first global producer and exporter of phosphate rock and its derivatives. The activities related to phosphate in Morocco are mainly focused on three areas: Khouribga, Gantour and Boucraâ. Phosphate transformation activities are essentially concentrated on Jorf Lasfar and Safi sites (Bentaleb, 2019). The phosphogypsum (PG), considered as a NORM (Naturally Occurring Radioactive Material (Cuesta et al., 2022)) waste, is generated during the production of phosphoric acid. Thus, phosphoric acid manufacturing units around the world produce about from 150 to 280 million tons of PG annually (Bouargane et al., 2023 a and b). It is estimated that about 5 tons of PG per ton of phosphoric acid (expressed as P_2O_5) are generated in the industrial process (El Zrelli et al., 2019). The chemical reaction for the digestion of fluorapatite may be expressed as follows (Perez-Moreno et al., 2019):

$$Ca_{10}(PO_4)_6F_{2(s)} + 10H_2SO_{4(l)} + 20H_2O_{(l)} \rightarrow 10CaSO_4{\cdot}2H_2O_{(s)} + 6H_3PO_{4(l)} + 2HF_{(aq)} \quad (1)$$

Due to the enormous amounts of PG, two main alternative management routes exist for the management of this by-product: (1) directly discharged into the sea, or (2) disposed of in stockpiles (Biyoune et al., 2021). Unfortunately, these management methods are often considered as the biggest environmental challenge of the phosphate industry. The storage of PG can produce a negative effect on groundwaters and surrounding soils (Bouargane et al., 2019). These waters and soils are very highly polluted with radionuclides and heavy metals which can cause a significant environmental impact (Lu et al., 2016). The waters contained in the PG piles present concentrations of natural radionuclides and heavy metals of about 3–4 orders of magnitude higher than those obtained for unperturbed surficial waters (Gaudry et al., 2007; Zairi and Rouis, 1999).

PG can be used as a source of Ca^{2+} and SO_4^{2-} to produce valuable materials in several fields (cement, plaster, agriculture…) (Abril et al., 2008; Harrou et al., 2020; Kacimi et al., 2006; Kuryatnyk et al., 2008;

* Corresponding author.
E-mail address: alejandro.barba@dci.uhu.es (A. Barba-Lobo).

https://doi.org/10.1016/j.ces.2023.119013
Received 6 March 2023; Received in revised form 27 May 2023; Accepted 14 June 2023
Available online 20 June 2023

Silva et al., 2021; Singh and Garg, 2005), as well as to be converted to: $CaCO_3$, Na_2SO_4, K_2SO_4, Li_2SO_4, $(NH_4)_2SO_4$, etc. (Altiner, 2018; Bouargane et al., 2020; Cárdenas-Escudero et al., 2011; El Alaoui-Belghiti et al., 2020; Ennaciri and Bettach, 2018; Idboufrade et al., 2021; Khachani et al., 2014).

A systematic review of various publications related to the PG field shows that this waste is of significant economic interest due to its high CaO and SO_3 content (Christophe et al., 2023; Bouargane et al., 2023b, Zdah et al. 2021). In many sites of the world there is natural gypsum (NG) in big amounts, and for that its price is very low. Only in areas characterized by having low NG, the PG valorization is interesting; this is a general idea. This makes PG potentially favorable on the one hand, for the mineral sequestration of CO_2, and on the other hand, for the production of value-added sulfates. In general, the perfect identification and characterization of the PG will strongly contribute to the good control of conversion of this by-product to valuable products, which is the goal of this work.

To the best of our knowledge, and although many papers have been published on PG carbonation by using alkaline reagents, very few papers there are in the literature about the behavior of toxic elements (As and heavy metals), and natural radionuclides (both ^{238}U- and ^{232}Th-series), specially evaluating the fluxes of the different species along the carbonation process. In addition, another main finding achieved in this study is the obtention of sulphates (X_2SO_4, where X = Na, K and NH_4) where the concentrations of pollutants are relatively small and, therefore, they can become a commercializable by-product.

For all reasons previously mentioned, this work aims to develop an attractive method for recycling and valorizing the Moroccan PG, by converting it into useful sulfates (X_2SO_4; X = Na, K or NH_4), portlandite ($Ca(OH)_2$) and calcium carbonate ($CaCO_3$), by using as alkaline reagent hydroxides of K, Na and NH_4. The characterization of these products can be applied to determine the carbonation efficiency of each alkali medium. Furthermore, this work also aims to evaluate the distribution of natural radionuclides, rare earth elements, metals and trace elements in the PG and the prepared compounds (Na_2SO_4, K_2SO_4, $(NH_4)_2SO_4$, $Ca(OH)_2$, $CaCO_3$) by the PG conversion.

2. Materials and methods

2.1. Chemicals and sampling

Sodium and potassium hydroxide (99%, Sigma-Aldric, Czech Republique), Ammonia (30%, Panreac, Spain), Synthetic gypsum SG (98%, LOBA Chemie, India) and deionized water were employed as reactants. The PG waste samples were collected from Jorf-Lasfar complex, Morocco.

2.2. Washing methodology

Pre-treatment by water-washing is widely used as effective and simple method of neutralization and removal of certain soluble impurities in various industries (Liu et al., 2019). The soluble impurities, salts or acids and organic matter not removed during the phosphoric acid (PA) production process, make the PG get a rather low pH, generally between 2 and 4. The PG water-washing process aims to reduce these impurities. The washing procedure is performed as follows: 10 g of PG are introduced into a beaker containing 20 mL of deionized water. To homogenize the solution, the whole is stirred magnetically for 20 min at an atmospheric pressure and a constant temperature of 25 °C. The washing procedure was repeated several times using the ratio of PG to water of 1:2 (Fig. 1).

2.3. Carbonation procedure

The experimental procedure was carried out as follows: dissolution of 10 g of PG in 400 mL of hydroxide aqueous solution (XOH, where X = K, Na or NH_4). The quantities of PG and XOH were weighted according to the stochiometric molar ratio of (OH^-: Ca^{2+}):

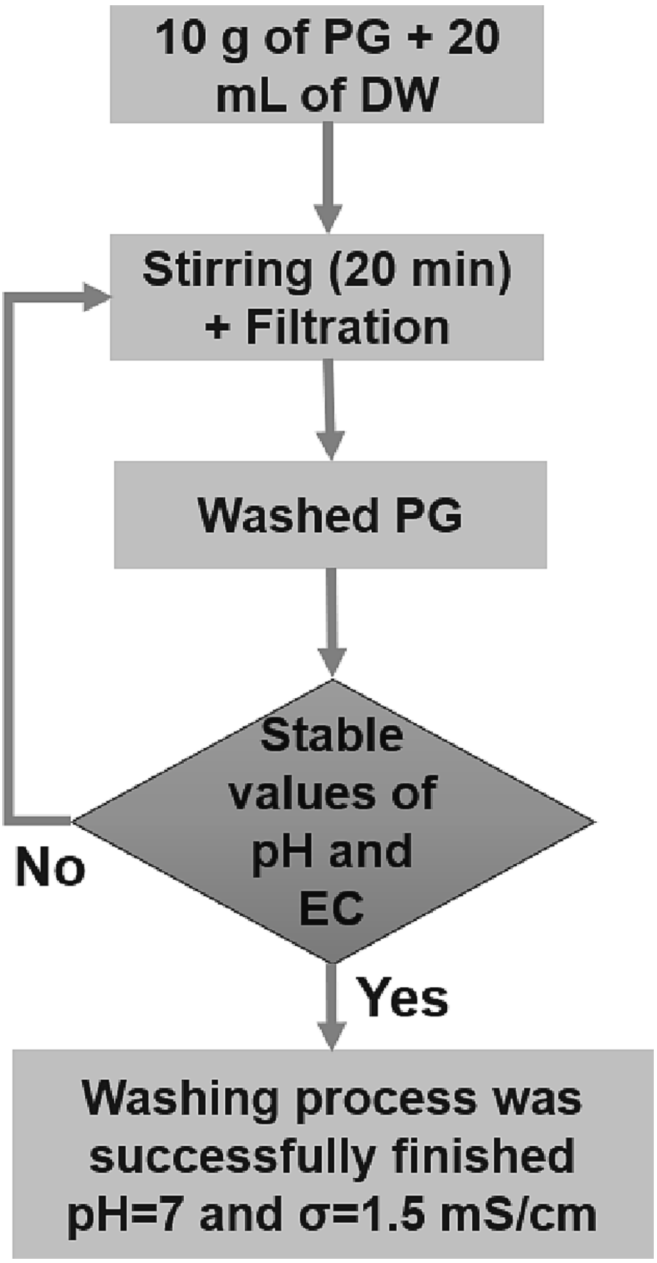

Fig. 1. PG washing process (DW: Distillated Water; EC: Electrical Conductivity (σ)).

- By dissolving the PG in KOH or NaOH solution, it is obtained the precipitation of a whitish solid phase named portlandite ($Ca(OH)_2$), which is recovered by filtration and fully dried at 40 °C. The evaporation of the supernatant at 80 °C, allowed us to obtain a second solid phase in the form of transparent salt (X_2SO_4):

$$CaSO_4{\cdot}2H_2O(s) + 2XOH(aq) \rightarrow Ca(OH)_2(s) + 2\,X^+(aq) + SO_4^{2-}(aq) + 2H_2O(l) \quad (2)$$

Then, the carbonation process was carried out by bubbling CO_2 flow in a portlandite solution (10 g/L) (El Housse et al. 2021a, 2021b, 2021c):

$$Ca(OH)_2(s) + CO_2(g) \rightarrow CaCO_3(s) + H_2O(l) \quad (3)$$

- On the other hand, the NH_4OH solution (0.6 M) was firstly neutralized by bubbling carbon dioxide to form ammonium carbonate $(NH_4)_2CO_3$ following the reaction (4) and then, 10 g of PG was added to the precedent solution (Eq. (5)):

$$2NH_4OH\ (aq) + CO_2\ (g) \rightarrow (NH_4)_2CO_3\ (aq) + H_2O\ (l) \quad (4)$$

$$CaSO_4{\cdot}2H_2O\ (s) + (NH_4)_2CO_3\ (aq) \rightarrow 2\ NH_4^+(aq) + SO_4^{2-}\ (aq) + CaCO_3\ (s) + 2H_2O\ (l) \quad (5)$$

The calcium carbonate was dried at 80 °C, and the evaporation of the obtained filtrate at 60 °C, allowing us to obtain $(NH_4)_2SO_4$.

2.4. Analytical and characterization techniques

X Ray Fluorescence: The identification and quantification of major elements contained in the solid samples were determined using a Panalytical brand X-ray fluorescence sequential spectrometer (AXIOS model) with a Rh tube was used. Prior to the analysis, the samples were prepared in the form of a tablet crushed by a manual press of the Retsch brand. The tablet was prepared on a boric acid bed. For this, 1.0 g of sample is homogeneously mixed with 0.06 g of wax, which acts as a binder. The XRF analysis was carried out by an accredited external laboratory, CITIUS (Center for Research, Technology and Innovation of the University of Sevilla).

X Ray Diffraction: The XRD patterns have been obtained with a Bragg-Brentano geometry powder X-ray diffractometer with Cu tube, Bruker brand equipment (model D8 Advance A25). A semi-quantitative method has been used, whose conditions were the following: $\Delta 2\theta$ = 3–70°; step = 0.015°; t = 0.1 s; tube conditions: 40 kV and 30 mA; divergence slit: fixed 0.5°; sample rotated at 30 rpm and nickel filter. The Diffrac Eva Phase Identification ("DIFFRAC.EVA" software) has been used in order to identify the crystalline phases, using the PDF-4 database (ICDD). The quantification has been carried out using the Rietveld method (Klika et al., 2020) (having employed the "DIFFRAC. TOPAS" software) in which zincite (ZnO) has been used as an internal standard, selecting a proportion of approximately 15% by weight, in order to determine the amorphous fraction. The XRD analysis was also carried out by CITIUS.

Inductively Coupled Plasma Mass Spectrometer: A 0.25 g sample were digested with four acids beginning with hydrofluoric, followed by a mixture of nitric and perchloric acids, heated using precise programmer-controlled heating in several ramping and holding cycles which takes the samples to incipient dryness. After incipient dryness was attained, samples were brought back into solution using aqua regia. The samples were then analyzed using an Inductively Coupled Plasma Mass Spectrometer (ICP-MS) Perkin Elmer Sciex ELAN 9000. Quality Control for the digestion is 14% for each batch, 5 method reagent blanks, 10 in-house controls, 10 samples duplicates, and 8 certified reference materials. An additional 13% QC is performed as part of the instrumental analysis to ensure quality in the areas of instrumental drift. The ICP-MS analysis were accomplished by Activation Laboratories (Actlabs), which is an accredited external laboratory placed in Canada.

Gamma-ray spectrometry: This radiometric technique is characterized by not being destructive, which allows us to measure the same sample as many times as desired. In order to proceed with the determination of the radionuclides present in a sample by using gamma-ray spectrometry, firstly it is necessary to dry the sample of interest at approximately 60 °C until constant weight. Secondly, the dried sample needs to be grinded and homogenized. Then, the dried sample mass is crushed until reaching the desired thickness (h). In our case, the selected geometry was cylindrical whose radius, r, is $r = 17.30(10)$ mm, where h and r are related to each other by $\rho = m/\pi r^2 h$, m and ρ being the mass and apparent density (or bulk density) of the dried sample, respectively.

Therefore, once the sample pretreatment has been carried out, it is ready to be measured. For this, an extended range high purity germanium detector (XtRa) was employed. Regarding the possible values that can be selected for h, these are ranged from 5 mm to 50 mm, since this detector was calibrated in efficiency varying the thickness of the calibration standards within the mentioned h range. The selected calibration standards were RGU-1, RGTh-1 and RGK-1, which are Certified Reference Materials (CRMs) provided by the IAEA (International Atomic Energy Agency). These CRMs contain only natural radionuclides from ^{238}U-series, ^{232}Th-series, and ^{40}K, respectively, whose certified activity concentrations are 4940 ± 15 Bq kg^{-1}, 3250 ± 45 Bq kg^{-1}, and 14000 ± 200 Bq kg^{-1}, respectively, where the uncertainties are given at 1 sigma level. For further information on this efficiency calibration, see Barba-Lobo et al., 2021. With respect to the characteristics of this detector, it has a relative efficiency of 38.4% (at 1332 keV (^{60}Co)) in relation to a NaI (Tl) detector with an active area of 3″ × 3″, a full width at half maximum (FWHM) of 1.74 keV and 0.88 keV at 1332 keV (^{60}Co) and 122 keV (^{57}Co), respectively, and a peak-Compton relation of 67.5:1. On the other hand, a conventional electronic chain is connected to the detector to obtain the gamma spectra by the Genie 2000 software. For further information on Genie 2000 software, see Zhu et al., 2009.

3. Results and discussion

3.1. PG washing process

During the PG washing process, 31 washing operations were performed. Fig. 2 presents the pH and electrical conductivity (EC) variations during the PG pre-treatment.

According to Fig. 2, a strong drop in electrical conductivity and a slight increase in pH can be observed from the first wash. This is due to the progressive elimination of acids from the soluble salts impregnated on the PG sample. Just after the fourth wash, the EC values drops from 4.31 to stabilize at about 2.1 mS cm^{-1}. In order to perform a comparative study between the dissolution behavior of PG and synthetic gypsum (SG) in distilled water, the pH and EC variation of a saturated solution of SG were represented on the same figure (Fig. 2). Towards the end of the PG washing process, the stabilization values of pH and conductivity of PG are closer to those of SG. They tend to the limit values of SG solution: 7 and 1.6 mS cm^{-1}, respectively.

As remarked in Fig. 2, the pH curves have two zones with different derivatives: 1) zone 1: pH = 3–4.5 and 2) zone 2: pH = 5.3–7.0. The zone 1 is related to P_2O_5 free dissolution, when the zone 2 represents the structural PG dissolution.

At the end of washing treatment process and basing on the PG solubility in distillated water (2.7 g/L (Hammas et al., 2013)), it is possible to conclude that at least, 10% of PG is dissolved. The washing process

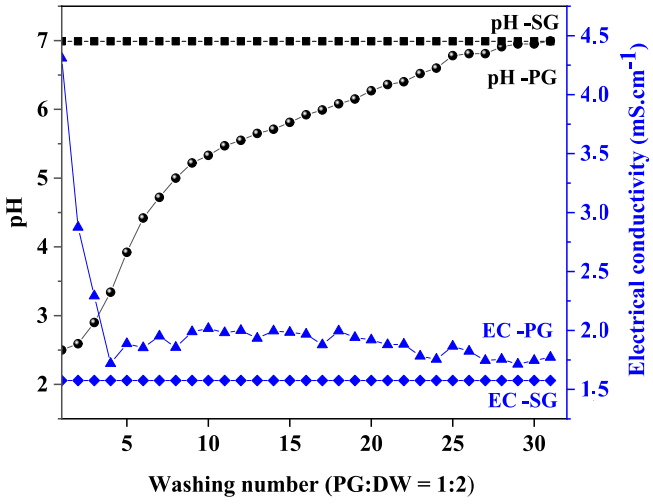

Fig. 2. Ph andelectrical conductivity (EC) measurement during the PG washing process (SG: synthetic gypsum).

presented here can be used as a guide and reference tool to describe the state of quality and purity of Moroccan PG. Depending on the PG application mode, it is possible to foresee the number of water-washing appreciable to eliminate the maximum of soluble impurities contained in the PG. On the other hand, the washing water can be systematically recycled for possible reuse in the industrial process of phosphate ore treatment.

3.2. PG characterization

3.2.1. XRF results

Table 1 shows the concentration (% weight) of the main major elements in both samples. A study of this table indicates that calcium and sulfur are the major elements constituting these products. They represent more than 70% of the overall composition of Moroccan PG. Similar results were obtained by Bourgier (2008). Silicon, phosphorus and fluorine are also found in low concentrations, as well as traces of: Al, Bi, Fe, K, Mg, Na, Nd, Sr, Ti and Y due essentially to the transfer of these impurities initially present in the Moroccan phosphate rock to the PG samples.

According to these results, and apart from a slight decrease in the content of minor elements Na, K and P, the PG water-washing process does not modify the original characteristics of the PG, in terms of major elements and mineral composition.

3.2.2. ICP-MS results

The ICP-MS (Table 2), show that the trace of starting PG is mainly composed of Sr, Ba, Cr and Mn. In general, trace element contents in PG can be attributed to many processes such as precipitation into a mineral phase, formation of solid solutions and adsorption to the surface of organic or inorganic compounds. In addition, unreacted phosphates and other impurities may be bound to the surface of PG crystals. The concentration levels of some elements contained in the Moroccan PG (i.e, Ba and Zn) are lower than those of the typical PG (Bourgier, 2008). With the exception of the content of Mo, Pb Zr, Sr and Cs, which can be considered as a similar concentration. The concentrations of other elements, such as Cd, Sr, Y and U, can be considered much higher than those of a typical PG (Mas et al., 2012; Bourgier, 2008). Considering the concentrations of these elements in both fresh and washed PG, it is remarkable that some elements such as Cr, Mn, and Sr, are partially dissolved in water.

In addition, the concentrations of most of the trace elements initially contained in the PG are present in concentrations above those typical of unperturbed soil, such as Ag, Cr, Cu, Pb and Zn, as in the fresh PG used in this work (Contreras et al., 2014).

Table 1
Major elements concentrations for studied PG (ND: not detected).

Major elements (%)	Fresh PG (this work)	Fresh PG (from bibliography (Rentería-Villalobos et al., 2010))	Washed PG (this work)
Ca	26 ± 2	27 ± 2	26 ± 2
S	16 ± 1	19 ± 9	16 ± 1
O	35 ± 2	36 ± 1	35 ± 2
P	0.35 ± 0.07	0.15 ± 0.01	0.25 ± 0.05
Si	0.27 ± 0.05	0.40 ± 0.01	0.26 ± 0.05
Al	0.07 ± 0.07	0.060 ± 0.001	0.07 ± 0.07
Fe	0.01 ± 0.01	0.01 ± 0.01	0.01 ± 0.01
Na	0.11 ± 0.02	0.17 ± 0.01	0.01 ± 0.01
K	0.01 ± 0.01	0.010 ± 0.001	< 0.01
Ti	0.02 ± 0.02	0.0100 ± 0.0004	0.02 ± 0.02
Mg	0.03 ± 0.02	< 0.01	0.01 ± 0.01
Sr	0.12 ± 0.02	0.15 ± 0.01	0.09 ± 0.09
Y	0.02 ± 0.02	< 0.01	0.02 ± 0.02
Bi	0.01 ± 0.01	< 0.01	ND
F	1.1 ± 0.1	< 0.01	1.2 ± 0.1
LOI	22	22	21

Table 2
Concentrations of PG trace elements (ppm).

Trace element (ppm)	Fresh PG This work	Washed PG This work	Fresh PG (Singh and Garg, 2005)	Unperturbed soil (Contreras et al., 2014)
Ag	1.5 ± 0.1	1.3 ± 0.1	ND	65
Ba	23 ± 5	19 ± 4	14 ± 3	ND
Cd	2.6 ± 0.5	0.8 ± 0.8	3 ± 1	0.09
Cr	16 ± 2	11 ± 3	14 ± 2	92
Cu	5.9 ± 1.2	2.9 ± 0.6	4 ± 1	28
Mn	8 ± 8	3.0 ± 3.0	ND	ND
Mo	0.95 ± 0.19	0.86 ± 0.17	ND	ND
Ni	1.2 ± 0.2	1.0 ± 0.2	ND	ND
Pb	1.7 ± 0.3	1.5 ± 0.3	2 ± 1	17
Se	1.1 ± 0.2	0.90 ± 0.90	ND	0.09
Sr	530 ± 27	474 ± 24	464 ± 20	348
Zn	3.0 ± 0.6	1.6 ± 0.3	4 ± 1	67

3.2.3. XRD results

The XRD patterns of fresh and washed PG samples are shown in Fig. 3. The diffraction pattern indicates that these samples are constituted mainly of gypsum ($CaSO_4{\cdot}2H_2O$, JCPDS file number: 96–101-1075), as expected (Cárdenas-Escudero et al., 2011). These results are consistent with the XRF measurements (Ca, S and O represent more than 70 wt%) and with those of the bibliography (Bourgier, 2008; Rentería-Villalobos et al., 2010). It can also be seen the presence of a very low intensity pattern (located around 28°) indicates the presence of quartz (SiO_2) as a minor impurity (JCPD file number: 01–081 0065) (El Alaoui-Belghiti et al., 2020). Moreover, the presence of quartz in the Moroccan PG can be explained as follows: (1) the Moroccan treated Phosphate ore is of sedimentary origin generally having higher SiO_2 contents and (2) SiO_2 is sometimes added to the liquor in the production of phosphoric acid to facilitate the crystallization process and to neutralize fluorine, sodium and/or potassium to form the compounds: H_2SiF_6, Na_2SiF_6 and K_2SiF_6. The analysis of the diffraction peaks reveals that the intensity corresponding to the (0 2 1) plane relative to the peak located at 11° is strongly accentuated (Fig. 3). It is thus possible to affirm that the crystals of Moroccan PG tend to orient themselves parallelly to this plane.

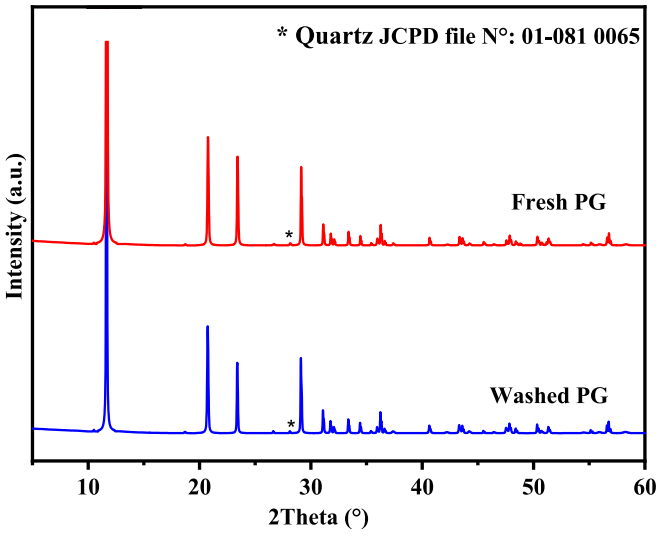

Fig. 3. XRD analysis patterns of fresh and washed PG.

Furthermore, the results from Fig. 3 confirm that the process adopted at Jorf Lasfar complex for the production of phosphoric acid is the dihydrate process. However, the hemihydrate process, which is relatively widespread in Europe, Japan and Africa, remains difficult to practice because the hemihydrate form of calcium sulfate tends to rehydrate again.

3.2.4. Gamma-ray spectrometry results

The PG used in this work presents: 113 ± 9 Bq kg^{-1}, 1097 ± 31 Bq kg^{-1} and 961 ± 41 Bq kg^{-1} for the activity concentrations in the case of the ^{238}U, ^{226}Ra and ^{210}Pb, respectively. It is important to note that the PG washing process did not decrease the concentrations of ^{238}U, ^{226}Ra and ^{210}Pb. In fact, the washed PG contains about 81 ± 1, 1071 ± 29 and 914 ± 42 Bq kg^{-1} respectively. Based on the literature, Moroccan PG has lower concentrations of ^{238}U, ^{226}Ra, and ^{210}Pb than Florida PG (Rutherford et al., 1996). However, these values are very close to those of the Spanish PG (Table 3).

3.3. PG conversion using hydroxide solutions (XOH)

3.3.1. pH-EC measurements during the conversion process

During the formation of the sulfate compounds (X_2SO_4), the changes in pH and EC can be explained on the basis of the following parts (Fig. 4a and c):

(1) Dissolving XOH in distilled water results in an alkaline mixture characterized by stabilization of pH and conductivity values.
(2) After the addition of PG to the XOH solution, two phenomena were observed: one corresponds to the dissolution of $CaSO_4{\cdot}2H_2O$ to give calcium ions, and the second corresponds to a decrease in OH^- ions that will combine with Ca^{2+} to precipitate as $Ca(OH)_2$ leading to a slight decrease in pH.
(3) The reaction (complexation/precipitation) is completed, since the values of the EC and pH remain stabilized.

When the carbonation reaction is based on CO_2 dissolution in portlandite solution and finally the CO_3^{2-} formation; this last one reacts with excess Ca^{2+} leading to the beginning of the carbonate solid phases' precipitation phenomena. For that, a sharp drop in pH is observed due essentially to the reduction of OH^- ions. Whereas the decrease in the conductivity values can be attributed to the consumption of Ca^{2+} and OH^- ions (Fig. 4b and 4d).

Concerning the dissolution of PG in NH_4OH, it is observed, after the addition of CO_2 at t ≈ 100 min (Fig. 4e), that the pH values decrease progressively (due to the neutralization of the basic solution (NH_4^+ + HO^-) by the carbonic acid ($CO_2 + H_2O$)). After two hours of agitation, the pH and conductivity values become stable. Indeed, calcium and sulfates ions coming from the dissolution of PG react with NH_4^+ and CO_3^- ions coming from neutralization to form $(NH_4)_2SO_4$ and $CaCO_3$.

Fig. 4 shows that the estimated time of the transformation of PG into marketable products vary considerably with the alkali solution type. The time required for the production of calcium carbonate from PG in the presence of Na^+, K^+ or NH_4^+ was found to be 60 min, 70 min and greater than 250 min, respectively (the reaction time was the time when both pH and EC values were stabilized).

Table 3
Concentration of PG radionuclides (Bq kg^{-1}).

Radionuclides		^{238}U	^{226}Ra	^{210}Pb
	Fresh PG	113 ± 9	1097 ± 31	961 ± 41
	Washed PG	81 ± 11	1071 ± 29	914 ± 42
From bibliography	**Morocco** (Borrego et al., 2007)	140	620	–
	Florida (Rutherford et al., 1996)	130	1140	1370
	Florida (Hull and Burnett, 1996)	From 225 to 1800		
	Spain (Tayibi et al., 2011)	102	520	881
	Tunisia (Tayibi et al., 2011)	31	188	163

*About 90–100% of the radioelements in the phosphate rock is fractionated to the PG.

3.3.2. Identification of the formed products

- ***Using NaOH reagent***

The conversion of PG into Na_2SO_4 and $CaCO_3$ takes place according to the following reactions (see Eqs. (6) and (7). In the experiment, 10 g of PG was used and the quantity of NaOH was added, in stoichiometric ratio (4.65 g), in 400 mL of distilled water (molar ratio: 1/1). During the experiment, $Ca(OH)_2$ was produced (4.10 g) and separated by filtration, while sodium and sulfates ions stayed in solution, according to the Eq. (6). Afterwards, the solution was evaporated to dryness and sodium sulfate formed (9.59 g). Then, 4 g of portlandite ($Ca(OH)_2$) were dispersed in 400 mL of distilled water under magnetic stirring into a thermostatic jacket, and a 20 mL min^{-1} CO_2 flow gas was injected to carry out the carbonation process (Eq. (7). Finally, about 3.84 g of solid were obtained.

$$CaSO_4{\cdot}2H_2O(s) + 2NaOH(aq) \rightarrow Ca(OH)_2(s) + 2Na^+(aq) + SO_4^{2-}(aq) + 2H_2O(l) \quad (6)$$

$$Ca(OH)_2(s) + CO_2(g) \rightarrow CaCO_3(s) + H_2O(l) \quad (7)$$

The multi-elemental and mineralogical characterizations of the samples obtained in the experiment have been shown below (Table 4 and Fig. 5). The formed solid by reaction of PG and NaOH, is composed of about 47.4% portlandite ($Ca(OH)_2$), but other minerals in lower proportion have also been presented, such as calcite (11%), gypsum (5%) and quartz (2%). These phases agree with the elemental composition measured by XRF, in which Ca was the major element contained in the sample. The other product obtained is characterized by the content of Na and S, agreeing with thenardite (62%), which was the main mineral phase found. However, other minority minerals were also found (calcite and burkeite). The presence of calcite and burkeite is due essentially to the contamination of portlandite with the atmospheric CO_2 (Khachani et al., 2014). On the other hand, the product obtained after the carbonation process consists almost entirely of calcite, as expected, its mineral composition being consistent with the elemental composition given by XRF. The mass of obtained calcite (3.84 g) confirms that the generated solid in the first reaction is not portlandite with high purity as indicated by the XRD analysis (Fig. 5), since in that case about 4.97 g should be obtained.

- ***Using KOH reagent***

The conversion of PG into K_2SO_4 and $CaCO_3$ takes place according to the following reactions. In the experiment, 10 g of PG were used, and the quantity of KOH was added, in stoichiometric ratio (6.50 g), in 400 mL of distilled water. During the experiment $Ca(OH)_2$ was produced (5.19 g) and separated by filtration, while potassium and sulfates ions stayed in solution, according to the Eq. (8). Afterwards, the solution was evaporated to dryness and potassium sulfate formed (9.87 g). Then, 4 g of portlandite ($Ca(OH)_2$) were dispersed in 400 mL of distilled water under magnetic stirring into a thermostatic jacket, and a 20 mL min^{-1} CO_2 flow gas was injected to carry out the carbonation process (Eq. (9). Finally, about 3.02 g of solid were obtained.

$$CaSO_4{\cdot}2H_2O(s) + 2KOH(aq) \rightarrow Ca(OH)_2(s) + 2K^+(aq) + SO_4^{2-}(aq) + 2H_2O(l) \quad (8)$$

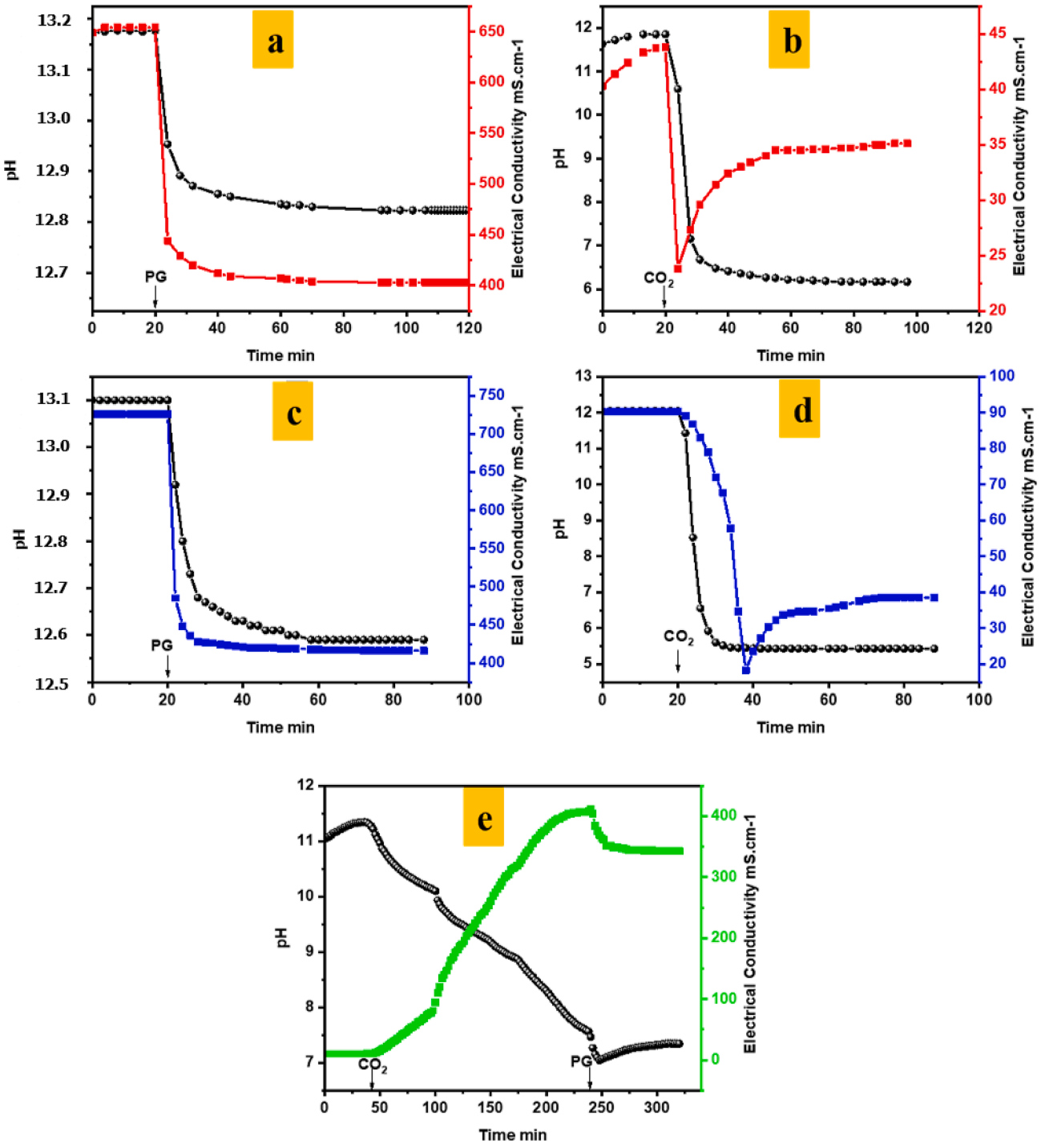

Fig. 4. pH and electrical conductivity variations during the conversion of PG to Na_2SO_4 and $CaCO_3$ (a and b), to K_2SO_4 and $CaCO_3$ (c and d) and to $(NH_4)_2SO_4$ and $CaCO_3$ (e).

$$Ca(OH)_2(s) + CO_2(g) \rightarrow CaCO_3(s) + H_2O(l) \quad (9)$$

The elemental and mineral characterizations of the samples obtained in the experiment were shown below (Table 5 and Fig. 6). The formed solid by reaction of PG and KOH, was mainly composed of about 40% and 26% of portlandite and gypsum, respectively, but other minerals in lower proportions were also presented, such as calcite (10%) and quartz (2%). The proportion of gypsum confirms the S content which was detected by XRF. Furthermore, the other mineral phases associated to the Ca agree with the high percentage of that element in the sample. The other product obtained is characterized by the content of K and S, agreeing with arcanite (34%), which was the main mineral phase found. However, other minority minerals were also detected (calcite and portlandite). The amorphous phase in K_2SO_4 phase is about 62%, that is due to the presence of amorphous salt of K_2SO_4 in this compound (Theo et al., 2004).

- ***Using NH_4OH reagent***

The conversion of PG into $(NH_4)_2SO_4$ and $CaCO_3$ takes place according to Eqs. (4) and (5). In the experiment, an ammonia solution (0.6

Table 4
Major elements and mineral composition during the PG conversion using NaOH solution.

Major elements (XRF)			
Elements (%)	$Ca(OH)_2$	Na_2SO_4	$CaCO_3$
Al	0.15 ± 0.03	0.10 ± 0.02	0.13 ± 0.03
Ca	48 ± 3	3.7 ± 0.2	39 ± 2
F	1.3 ± 0.1	< 0.01	1.0 ± 0.1
Fe	0.02 ± 0.02	0.01 ± 0.01	0.02 ± 0.02
K	< 0.01	0.04 ± 0.04	< 0.01
Mg	0.01 ± 0.01	< 0.01	0.01 ± 0.01
Na	0.42 ± 0.08	26 ± 2	0.05 ± 0.05
P	0.59 ± 0.12	< 0.01	0.49 ± 0.10
S	1.6 ± 0.1	18 ± 1	0.50 ± 0.10
Si	0.53 ± 0.11	2.6 ± 0.1	0.63 ± 0.13
Sr	0.05 ± 0.05	0.05 ± 0.05	0.03 ± 0.03
Ti	0.03 ± 0.03	< 0.01	0.03 ± 0.03
Y	0.04 ± 0.04	< 0.01	0.03 ± 0.03
LOI	24	8.1	41
Mineral composition (%)			
Thenardite (Na_2SO_4)	ND	62 ± 7	ND
Portlandite ($Ca(OH)_2$)	47 ± 1	ND	ND
Calcite ($CaCO_3$)	11 ± 1	4.0 ± 0.4	97 ± 2
Burkeite ($Na_6(CO_3)(SO_4)_2$)	ND	1.4 ± 0.4	ND
Gypsum ($CaSO_4{\cdot}2H_2O$)	5.4 ± 0.8	ND	ND
Quartz (SiO_2)	2.4 ± 0.1	ND	3.4 ± 0.1
Amorphous	34 ± 2	32 ± 7	ND

M) was put in contact with bubbly CO_2 to form ammonium carbonate, according to the Eq. (4). Then, 10 g of PG were added. During the experiment, $CaCO_3$ was produced (5.97 g) and separated by filtration, while ammonium and sulfates ions stayed in solution (Eq. (5). Afterwards, the solution was evaporated to dryness and ammonium sulfate was formed (7.63 g).

The elemental and mineral characterizations of the samples obtained in the experiment were shown below (Table 6). The formed solid by reaction of PG and $(NH_4)_2CO_3$, was calcite with a purity of 96.8%, which was determined by the XRD analysis (Fig. 7). This value agreed with the Ca concentration found by XRF. The other product obtained was identified as mascagnite (100%), as expected.

3.4. Trace elements distribution during the conversion procedures

Because of their speed and ease of use, the two main analytical techniques, XRF and ICP-MS, were used to determine predominantly or trace elements present in the portlandite, sulfates and carbonates compounds obtained during PG conversion. In all cases, trace elements refer to elements present at very small concentrations (<100 ppm), and they can be subsets of heavy metals, i.e., elements that have high densities and toxicities.

To study the distribution of elements during the dissolution of PG in alkali mediums and the carbonation process, the transfer factor (F_T) is most frequently used. It represents the fraction of each element transferred into each of the products compared to the initial value contained in all the reactants. The F_T factor can be known by the following equation (Contreras et al., 2014):

$$\mathbf{F_T(i)} = \frac{\mathbf{Cp(i)*mp}}{\sum \mathbf{Cr(i)*mr}} \times 100 \qquad (10)$$

Where:

- $C_p(i)$ and $C_r(i)$ are respectively, the concentrations of element (i) in the products and reactants for each reaction;
- m_r and m_p are respectively, the amount of the reactants used and of the product obtained for each reaction. In other words, they are the masses experimentally involved in the chemical reaction.

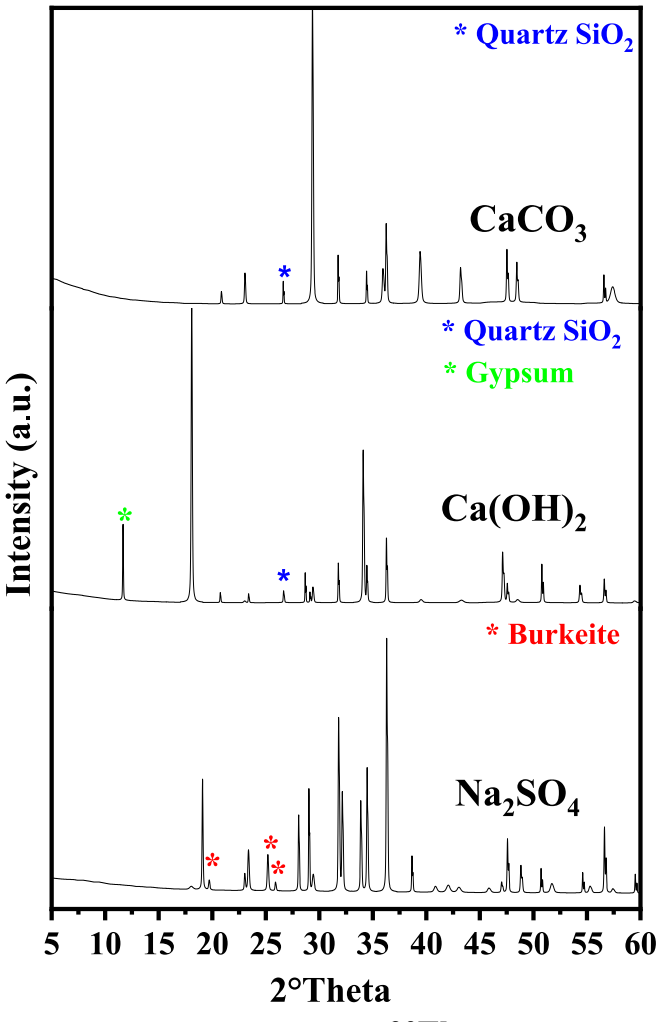

Fig. 5. Diffractograms patterns of the formed products: *Na_2SO_4, $Ca(OH)_2$ et $CaCO_3$.*

Table 5
Major elements and mineral composition during the PG conversion using KOH solution.

Major elements (XRF)			
Elements (%)	$Ca(OH)_2$	K_2SO_4	$CaCO_3$
Al	0.14 ± 0.03	0.03 ± 0.03	0.16 ± 0.03
Ca	42 ± 3	3.5 ± 0.2	39 ± 2
F	1.3 ± 0.1	< 0.01	1.1 ± 0.1
Fe	0.01 ± 0.01	0.01 ± 0.01	0.02 ± 0.02
K	0.65 ± 0.13	46 ± 3	0.07 ± 0.07
Mg	0.01 ± 0.01	< 0.01	0.01 ± 0.01
Na	0.02 ± 0.02	0.33 ± 0.07	0.02 ± 0.02
P	0.52 ± 0.10	< 0.01	0.59 ± 0.12
S	4.7 ± 0.2	10 ± 1	1.4 ± 0.1
Si	0.53 ± 0.11	1.1 ± 0.1	0.63 ± 0.13
Sr	0.06 ± 0.06	0.07 ± 0.07	0.04 ± 0.04
Ti	0.03 ± 0.03	< 0.01	0.04 ± 0.04
Y	0.04 ± 0.04	< 0.01	0.04 ± 0.04
LOI	24	13	38
Mineral composition (%)			
Arcanite (K_2SO_4)	ND	34 ± 1	ND
Portlandite ($Ca(OH)_2$)	40 ± 2	0.4 ± 0.3	8.0 ± 1.3
Calcite ($CaCO_3$)	10 ± 1	2.8 ± 0.7	81 ± 2
Gypsum ($CaSO_4{\cdot}2H_2O$)	26 ± 1	ND	1.6 ± 0.1
Bassanite ($CaSO_41/2H_2O$)	ND	ND	1.6 ± 0.1
Quartz (SiO_2)	1.1 ± 1.0	ND	2.9 ± 0.1
Amorphous	24 ± 2	63 ± 2	5.0 ± 2.0

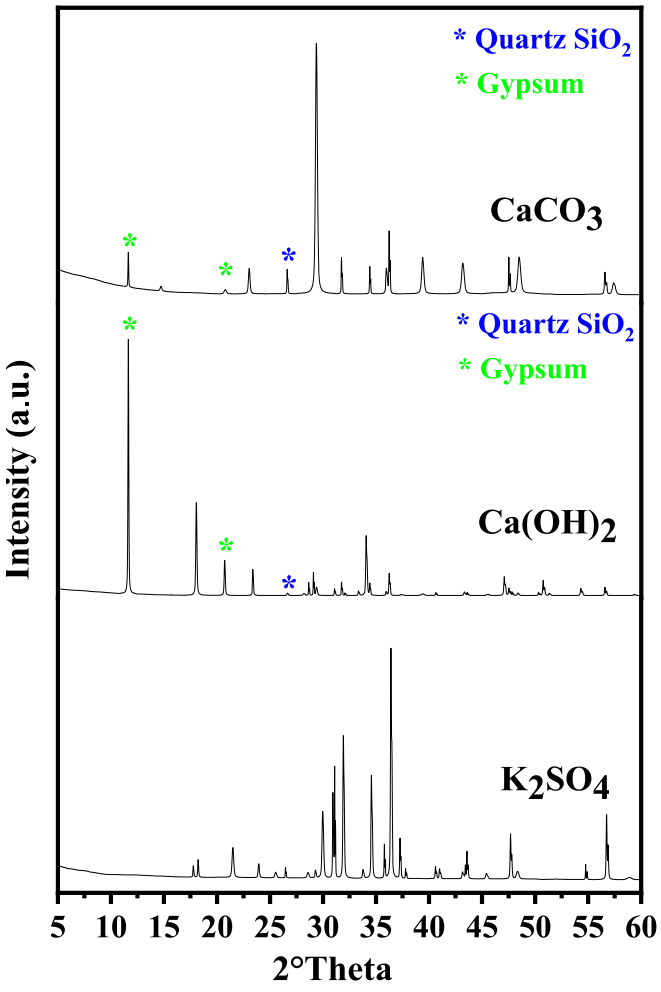

Fig. 6. Diffractograms patterns of the formed products: K_2SO_4, $Ca(OH)_2$ and $CaCO_3$.

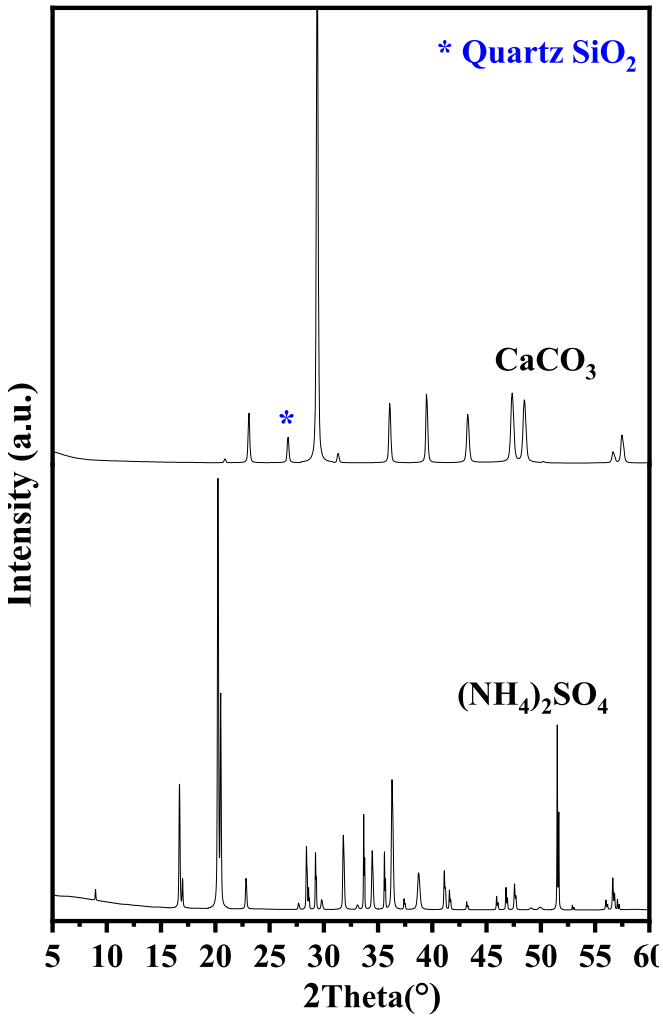

Fig. 7. Diffractograms patterns of the formed products: $(NH_4)_2SO_4$ and $CaCO_3$.

Table 6
Major elements and mineral composition during the conversion of PG into $(NH_4)_2SO_4$ and $CaCO_3$.

Major elements (XRF)		
Elements (%)	$(NH_4)_2SO_4$	$CaCO_3$
Al	ND	0.10 ± 0.02
Ca	0.70 ± 0.14	39 ± 2
F	0.39 ± 0.08	1.00 ± 0.05
Fe	0.01 ± 0.01	0.01 ± 0.01
K	0.02 ± 0.02	< 0.01
Mg	0.02 ± 0.02	0.01 ± 0.01
Na	0.08 ± 0.08	0.02 ± 0.02
P	0.20 ± 0.04	0.31 ± 0.06
O	59 ± 3	17 ± 1
S	39 ± 2	0.55 ± 0.11
Si	0.20 ± 0.04	0.33 ± 0.07
Sr	0.01 ± 0.01	0.12 ± 0.02
Ti	< 0.01	0.03 ± 0.03
Y	< 0.01	0.03 ± 0.03
LOI	99.1	41.45
	Mineral composition (%)	
Mascagnite ($(NH_4)_2SO_4$)	100 ± 7	ND
Calcite ($CaCO_3$)	ND	97 ± 2
Quartz (SiO_2)	ND	1.7 ± 0.2
Amorphous	ND	1.5 ± 1.4

In the case of NaOH reactant and according to the XRF (Table 4) and ICP-MS data (Table 7), 78% of the calcium (Ca) was transferred from PG to portlandite, then 77% from portlandite to the final compound calcite. Other elements such as: Al, Y, S and P were also fully transferred to portlandite and by subsequent carbonation to calcite. On the other hand, most of the sulfur (S) (>100%) initially present in the PG was partitioned, along with sodium (Na) (94%) from NaOH, into the thenardite (Na_2SO_4). Generally, an increasing in the concentrations of portlandite and calcite was observed (Table 4), this generates a high transfer factor. Logically, the dissolution of PG and the precipitation of portlandite and/or calcite involve a loss of mass. This consequently leads to an increase in the concentration of contaminants. Thus, during alkaline dissolution of PG, F_T analysis shows two types of behavior:

- Preservative: several elements have shown a very high transfer factor to the solid phase like Ag, Ba, Se, Ca, Mg, F, P, Si, Ti or Y. They tend to precipitate and/or adsorb more or less in the solid phase $Ca(OH)_2$.
- Non-conservative: minor elements such as Cr, Cu, Mn, Mo or Ni and major elements such as K, Na or S, migrate preferentially to the liquid phase.

Considering the KOH case and according to Table 5, the major elements (Ca and S) were transferred to portlandite, arcanite, and calcite in the following percentages (F_T calculated using the Eq. (10) and Table 5 values):

Table 7
Trace elements concentrations (ppm) and transfer factor (F_T) during the conversion procedures.

PG dissolution $CaSO_4{\cdot}2H_2O_{(s)} + 2NaOH_{(aq)} \rightarrow Ca(OH)_{2(s)} + Na_2SO_{4(aq)} + 2H_2O_{(l)}$					**Carbonation** $Ca(OH)_{2(s)} + CO_{2(g)} \rightarrow CaCO_{3(s)} + H_2O_{(l)}$			
Trace elements (ICP-MS)								
Element (ppm)	**PG (10 g)**	**NaOH (4,65 g)**	**$Ca(OH)_2$ (4,1 g)**	**F_T (%)**	**Na_2SO_4 (9,59 g)**	**F_T (%)**	**$CaCO_3$ (3,84 g)**	**F_T (%)**
Ag	1.3 ± 0.1	10	19 ± 1	~100	2.3 ± 0.1	37	53 ± 3	~100
Ba	19 ± 4	–	62 ± 12	~100	7 ± 7	35	124 ± 6	~100
Cd	0.80 ± 0.80	50	2.3 ± 0.5	3.9	< 0.1	0.40	2.2 ± 0.4	92
Cr	11 ± 3	–	13 ± 3	49	< 1	ND	18 ± 4	~100
Cu	2.9 ± 0.6	–	5.6 ± 1.1	79	< 0.2	ND	5.7 ± 1.1	89
Mn	3 ± 3	–	7.0 ± 7.0	96	< 1	ND	5 ± 5	69
Mo	0.86 ± 0.17	–	0.90 ± 0.20	60	0.54 ± 0.11	43	0.55 ± 0.11	59
Ni	1.0 ± 0.2	10	4.3 ± 0.9	31	< 0.5	ND	4.3 ± 0.9	96
Pb	1.5 ± 0.3	10	4.3 ± 0.9	~100	< 0.5	ND	4.6 ± 0.9	~100
Se	0.9 ± 0.9	–	1.7 ± 0.3	77	0.3 ± 0.3	32	1.4 ± 0.3	79
Sr	474 ± 24	–	388 ± 19	62	< 0.2	ND	258 ± 13	64
Zn	1.6 ± 0.3	50	2.0 ± 0.4	96	12 ± 1	48	3.9 ± 0.8	~100

PG dissolution $CaSO_4{\cdot}2H_2O_{(s)} + 2KOH_{(aq)} \rightarrow Ca(OH)_{2(s)} + K_2SO_{4(aq)} + 2H_2O_{(l)}$					**Carbonation** $Ca(OH)_{2(s)} + CO_{2(g)} \rightarrow CaCO_{3(s)} + H_2O_{(l)}$			
Trace elements (ICP-MS)								
Element (ppm)	**PG (10 g)**	**KOH (4.65 g)**	**$Ca(OH)_2$ (5.19 g)**	**F_T (%)**	**K_2SO_4 (9.87 g)**	**F_T (%)**	**$CaCO_3$ (3.02 g)**	**F_T (%)**
Ag	1.3 ± 0.1	10	5.3 ± 0.3	46	2.2 ± 0.1	37	8.6 ± 0.4	~100
Ba	19 ± 4	–	63 ± 13	~100	7 ± 7	36	86 ± 17	~100
Cd	0.8 ± 0.8	50	1.9 ± 0.4	4.1	< 0.1	0.41	2.6 ± 0.5	~100
Cr	11 ± 3	–	9.0 ± 1.8	43	< 1	ND	13 ± 3	~100
Cu	2.9 ± 0.6	–	5.2 ± 1.0	93	< 0.2	ND	6.5 ± 1.3	94
Mn	3 ± 3	–	4 ± 4	69	15 ± 3	66	5 ± 5	94
Mo	0.86 ± 0.17	–	0.8 ± 0.2	49	< 0.05	ND	0.68 ± 0.10	63
Ni	1.0 ± 0.2	10	2.1 ± 0.4	19	16 ± 1	51	3.9 ± 0.8	~100
Pb	1.5 ± 0.3	10	3.9 ± 0.8	33	4.5 ± 0.9	70	5.1 ± 1.0	99
Se	0.9 ± 0.9	–	1.4 ± 0.3	81	< 0.1	11	1.6 ± 0.3	86
Sr	474 ± 24	–	422 ± 22	46	< 0.2	ND	350 ± 18	48
Zn	1.6 ± 0.3	50	1.5 ± 0.3	3.1	10 ± 2	39	4.5 ± 0.9	~100

PG dissolution and carbonation $CaSO_4{\cdot}2H_2O_{(s)} + 2NH_4OH_{(aq)} + CO_{2(g)} \rightarrow (NH_4)_2SO_{4(aq)} + CaCO_{3(s)} + H_2O_{(l)}$						
Trace elements (ICP-MS)						
Element (ppm)	**PG (10 g)**	**NH_4OH (10.2 g)**	**$(NH_4)_2SO_4$ (9.87 g)**	**F_T (%)**	**$CaCO_3$ (3.02 g)**	**F_T (%)**
Ag	1.3 ± 0.1	0.1	< 0.05	ND	6.8 ± 0.3	~100
Ba	19 ± 4	0.1	4 ± 4	<1	94 ± 19	~100
Cd	0.8 ± 0.8	0.1	< 0.1	ND	1.8 ± 0.4	~100
Cr	11 ± 3	0.05	18 ± 4	24	11 ± 2	70
Cu	2.9 ± 0.6	0.1	3.5 ± 0.7	<1	3.8 ± 0.8	~100
Mn	3 ± 3	0.1	8. ± 2	3	4 ± 4	96
Mo	0.86 ± 0.17	0.02	0.36 ± 0.07	11	0.86 ± 0.17	47
Ni	1.0 ± 0.2	0.05	< 0.5	ND	1.8 ± 0.4	~100
Pb	1.5 ± 0.3	0.05	2.4 ± 1.5	<1	3.4 ± 0.7	~100
Se	0.9 ± 0.9	–	< 0.1	3	1.3 ± 0.3	~100
Sr	474 ± 24	1	20 ± 4	15	> 1000	~100
Zn	1.6 ± 0.3	0.1	3.1 ± 1.2	<1	1.3 ± 0.3	~100

- Calcium: 87% for portlandite and 88% for calcite,
- Sulfur: 99% for arcanite.

Other elements such as Al, Fe, Si and Sr were also fully transferred to calcite (Table 7). From these results, it can be deduced that most of the trace elements prefer to move from PG to portlandite and then to the synthesized calcium carbonate. This can be explained by the chemical behavior of some elements which is similar to that of calcium.

3.5. Radioelements distribution during the conversion procedures

In this section, it has been carried out a study on the behavior of the radionuclides during the conversion procedures. For this, ^{238}U (via ^{234}Th (63 keV)), ^{226}Ra (via ^{214}Pb (352 keV)) and ^{210}Pb (46 keV) have been determined by gamma-ray spectrometry for the washed PG, as well as the products obtained (portlandite, calcite and sulfates (X_2SO_4, where X = Na, K or NH4)). This study allows us to know how the radionuclides are distributed during the conversion of PG into X_2SO_4 and $CaCO_3$.

For all samples, the time elapsed between the sample preparation and its measurement was at least 1 month, where it is well known that this time interval is proper in order to get secular equilibrium between ^{226}Ra and ^{222}Rn. Furthermore, the calculations of the ^{226}Ra concentrations were carried out by using its gamma emission (186 keV) and their daughters (^{214}Pb and ^{214}Bi), obtaining results statistically compatible. This proves that when the samples were measured, the ^{226}Ra and ^{222}Rn were in secular equilibrium.

In the case of the washed PG, the calculated activity concentrations were 81 ± 11 Bq kg^{-1}, 1097 ± 31 Bq kg^{-1} and 914 ± 42 Bq kg^{-1} for ^{238}U, ^{226}Ra and ^{210}Pb, respectively, while for the raw PG, the obtained activity concentrations were 113 ± 9 Bq kg^{-1}, 1071 ± 29 Bq kg^{-1} and 961 ± 41 Bq kg^{-1} for ^{238}U, ^{226}Ra and ^{210}Pb, respectively.

Taking the Eq. (10) into account, it is possible to know the F_T for all the formed compounds and, consequently, the distribution of the three radionuclides (^{238}U, ^{226}Ra and ^{210}Pb), is completely known. Therefore, the obtained F_T values have been shown in the Figure below (Fig. 8) for the different compounds ($CaCO_3$ and X_2SO_4) and radionuclides (^{238}U, ^{226}Ra and ^{210}Pb). Thus, considering the NaOH reagent, the obtained F_T values for calcite were 99 ± 15% and 99 ± 6% in the case of ^{238}U and ^{210}Pb, respectively, while F_T was 96 ± 3% in the case of ^{226}Ra. This fact suggest that most radionuclides are transferred to the calcite product. Note that the F_T associated to the portlandite has not been considered.

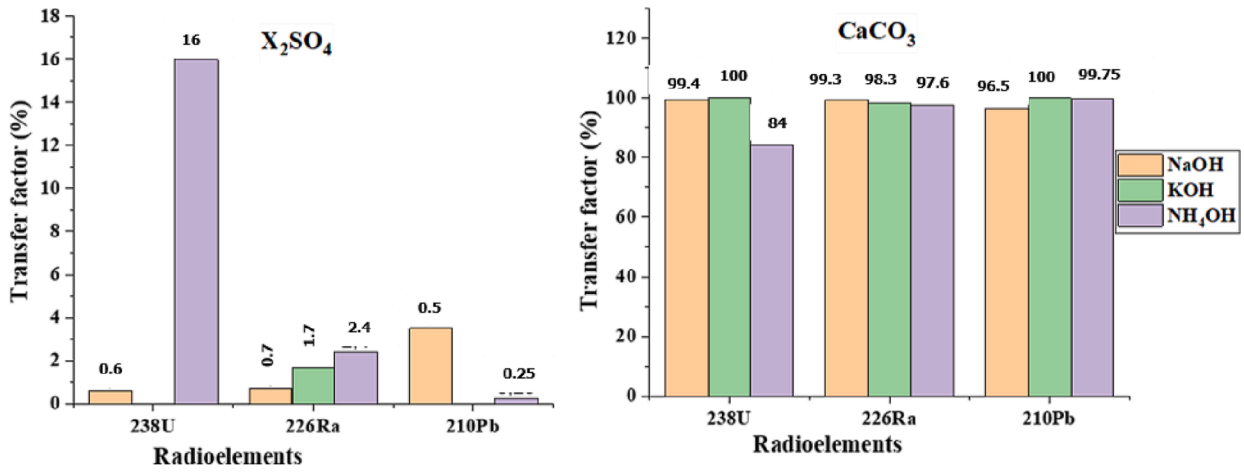

Fig. 8. Radioelements distribution during the conversion of PG into X_2SO_4 and $CaCO_3$.

The reason is because the portlandite behaves as an intermediate in the reactions described by Eqs. (6) and (7). On the other hand, in the cases related to the KOH reagent, it is possible to observe that the sum of the calcite and sulfate F_T values did not reach 100% for any radionuclides. Consequently, the obtained F_T values differ from 100%, this being especially true for ^{226}Ra and ^{210}Pb. In order to discard possible issues related to the chemical composition of the K_2SO_4 sample, the activity concentration of ^{40}K was calculated, obtaining 13189 ± 555 Bq kg^{-1}. Therefore, taking the relation established by the IAEA, which says that 1% of natural K is equivalent to 313 Bq kg^{-1} of ^{40}K, a percentage of 42.3 ± 1.9% was obtained of natural K in the case of the K_2SO_4 sample. This is very consistent with the K proportion obtained by XRF analysis for this sample, this proportion being 46 ± 2%.

Regarding the cases resulted from the NH_4OH reagent, the F_T values obtained for ^{238}U, ^{226}Ra and ^{210}Pb were 84 ± 12%, 98 ± 3% and 100 ± 6% for the calcite, respectively, while in the case of the sulfate, the obtained F_T values were 16 ± 3%, 2.40 ± 13% and 0.25 ± 17%, respectively. Taking these percentages into account, it is possible to realize that the total F_T values were close to 100%, this being especially true for ^{210}Pb. Therefore, the conversion procedures of PG into $(NH_4)_2SO_4$ and $CaCO_3$ were accomplished in a proper way.

3.6. Carbonation efficiency

In general, mineral carbonation represents a promising and effective option for storing carbon dioxide in a solid form (Ramli et al., 2021). In our case, it is the reaction of CO_2 with bivalent cations Ca^{2+} from the dissolution of PG, forming stable carbonates. In the carbonation procedure, approximately 4 g of portlandite were dispersed in 400 mL of distilled water. About 3.84, 3.02 and 3.97 g of solid calcite is finally obtained using NaOH, KOH and NH_4OH, respectively. The carbonation efficiency (CE) can be evaluated by considering the theoretical and the experimental amount of calcite that should be formed (in g). Therefore, the CE can be defined as a mathematical relationship written as follow:

$$\boldsymbol{CE}(\%) = 100\frac{\boldsymbol{m_e}\left(\frac{\boldsymbol{P_e}}{100}\right)}{\boldsymbol{m_t}} \quad (11)$$

With:

- m_t is the theoretical mass of calcite calculated based on the total carbonation reaction of portlandite:

$$Ca(OH)_{2(s)} + CO_{2(g)} \rightarrow CaCO_{3(s)} + H_2O_{(l)} \quad (12)$$

- m_e is the experimental mass of calcite;
- Pe is the purity of the calcite formed, which was previously determined using mineralogical analysis obtained by XRD.

Table 8
Carbonation efficiency (%).

Mineral	m_t(g)	m_e(g)	P_e(%)	CE (%)
PG (25.6% Ca)	10.00	–	–	–
$CaCO_3$ (NaOH)	6.41	3.84 ± 0.01	97 ± 2	58 ± 9
$CaCO_3$ (KOH)	6.41	3.02 ± 0.01	81 ± 2	38 ± 5
$CaCO_3$ (NH_4OH)	6.41	5.97 ± 0.01	97 ± 2	90 ± 2

The m_t, m_e and the CE values are displayed in the table below (Table 8):

From the Table 8, it is clear that the presence of NH_4^+ in the solution improved the carbonation efficiency (90%). The CE was 58% and 38% in the presence of Na^+ and K^+, respectively.

Based on the conversion reactions (Eq (4) to (9), Table 8 and our recently published article (Bouargane et al., 2023a), the amount of CO_2 used for each reagent, using 1 t of PG, is summarized as follows:

- Using NaOH reagent: to produce 0.6 t of $CaCO_3$, about 0.25 t of CO_2 was needed. According to Fig. 4a and b, this step will be completed within 60 min;
- Using KOH reagent: to produce 0.58 t of $CaCO_3$, about 0.2 t of CO_2 was needed. According to Fig. 4c and d, this step will be completed within 70 min;
- Using NH_4OH reagent: to produce 0.58 t of $CaCO_3$, about 0.25 t of $CO_2$was needed. According to Fig. 4f, this step will be completed within 250 min;

Based on the annual production of PG (about 150 to 280 million tons) and CO_2, considered the main greenhouse gas emission, the carbonatation processes of PG in hydroxide aqueous mediums could be utilized as a promising method for carbon capture and sequestration to produce a calcium carbonate, $CaCO_3$, with significant market value, besides other value-added products (Mattila et al. 2015).

The preliminary results obtained for this step are interesting due to the simplicity of the proposed process. Generally, carbonation by aqueous route is more promising than the thermal route (Baciocchi et al., 2010). Indeed, the CO_2 dissolves in the aqueous phase and induces the acidification of the reaction medium which considerably improves the speed of mineral carbonation.

4. Conclusions

The study presented in this paper aims to address the environmental problems associated with the large annual production of PG. Three PG carbonation methods were studied by using different alkaline media (XOH). The conversion reactions of PG were monitored by measuring the pH and conductivity values of the corresponding solutions simultaneously. The different analyses carried out on the Moroccan PG show that this waste presents an important economic interest because of its high content of calcium and sulfate. This makes the PG potentially favorable on the one hand, for the mineral sequestration of CO_2 which leads to the formation of calcium carbonate, and on the other hand, for the production of value-added sulfate compounds; X_2SO_4 (X = Na, K or NH_4).

As for the trace impurities initially contained in the PG, most of these elements were found to be completely transferred into the final calcite. Indeed, and with the exception of the elements K, P, S, Na and N the majority of the other elements show a conservative behavior towards calcite during the carbonation process. It should be noted that silica (SiO_2), initially presents as an insoluble impurity in the starting PG, is successively transferred to portlandite and then to calcite. Nevertheless, the calcite thus synthesized, is highly recommended for the production of cement whose main constituent, the clinker, is obtained by the firing of calcium carbonate, silica, alumina and iron oxide.

In addition, the main advantage of this process is that it avoids the formation of secondary salts such as syngenite ($K_2SO_4{\cdot}CaSO_4{\cdot}H_2O$) and penta-salt ($K_2SO_4{\cdot}5CaSO_4{\cdot}H_2O$) during the conversion of PG into potassium sulfate in the presence of KOH.

The gamma-ray spectrometry method allowed us to evaluate the distribution of the radioactive elements ^{238}U, ^{226}Ra and ^{210}Pb during the conversion of PG. Indeed, the concentrations found in the sulfates synthesized (X_2SO_4) are generally very negligible compared to those contained in the starting PG. Moreover, these salts seem to be of high purity. The particular beneficial aspect of these procedures is the preferential accumulation of the different radionuclides ^{238}U, ^{226}Ra and ^{210}Pb in the calcite. Moreover, calcite is much more soluble than PG in acidic media, which favors the recovery of both rare earth elements and radioelements.

5. Statements and declarations

Ethical Approval.

This study does not involve animal or human subjects.

Consent to Participate.

All authors agreed with the content and all gave explicit consent to submit and they obtained consent from the responsible authorities at the institute/organization where the work has been carried out, before the work is submitted.

Consent to Publish.

The authors have no financial or proprietary interests in any material discussed in this article.

Funding.

Funding for open access charge: Universidad de Huelva / CBUA.

Availability of data and materials.

All data and materials as well as software application or custom code support their published claims and comply with field standards.

CRediT authorship contribution statement

Brahim Bouargane: Conceptualization, Data curation, Formal analysis, Investigation, Methodology, Validation, Writing – original draft, Writing – review & editing. **Silvia M. Pérez-Moreno:** Conceptualization, Data curation, Formal analysis, Investigation, Methodology, Validation, Writing – original draft, Writing – review & editing. **Alejandro Barba-Lobo:** Conceptualization, Data curation, Formal analysis, Investigation, Methodology, Validation, Writing – original draft, Writing – review & editing. **Bahcine Bakiz:** Conceptualization, Data curation, Formal analysis, Investigation, Methodology, Supervision, Validation, Writing – original draft, Writing – review & editing. **Ali Atbir:** Conceptualization, Data curation, Formal analysis, Investigation, Methodology, Supervision, Validation, Writing – original draft, Writing – review & editing. **Juan Pedro Bolívar:** Conceptualization, Data curation, Formal analysis, Investigation, Methodology, Supervision, Validation, Writing – original draft, Writing – review & editing.

Declaration of Competing Interest

The authors declare that they have no known competing financial interests or personal relationships that could have appeared to influence the work reported in this paper.

Data availability

Data will be made available on request.

References

Abril, J.M., García-Tenorio, R., Enamorado, S.M., Hurtado, M.D., Andreu, L., Delgado, A., 2008. The cumulative effect of three decades of phosphogypsum amendments in reclaimed marsh soils from SW Spain: ^{226}Ra, ^{238}U and Cd contents in soils and tomato fruit. Sci. Total Environ. 403 (1–3), 80–88. https://doi.org/10.1016/j.scitotenv.2008.05.013.

Altiner, M., 2018. Effect of alkaline types on the production of calcium carbonate particles from gypsum waste for fixation of co$_2$ by mineral carbonation. Int. J. Coal Prep. Util. 39 (3), 1–19. https://doi.org/10.1080/19392699.2018.1452739.

Baciocchi, R., Costa, G., Di Bartolomeo, E., Polettini, A., Pomi, R., 2010. Carbonation of stainless steel slag as a process for CO_2 storage and slag valorization. Waste and Biomass Valorization 1 (4), 467–477. https://doi.org/10.1007/s12649-010-9047-1.

Barba-Lobo, A., Mosqueda, F., Bolívar, J.P., 2021. An upgraded lab-based method to determine natural γ-ray emitters in NORM samples by using Ge detectors. Measurement 186, 110153. https://doi.org/10.1016/j.measurement.2021.110153.

Bentaleb, M.A.,"Implementing circular economy strategies in Morocco," *Sch. Sci. Eng. – Al Akhawayn Univ.*, no. April, 2019.

Biyoune, M.G., Bouargane, B., Idboufrade, A., Marrouche, A., Atbir, A., Boukbir, L., Mançour-billah, S., 2021. New procedure for water-salinity reduction using Phosphogypsum waste and carbon dioxide resulting inuseful compounds formation. Nanotechnol. 6 (2).

Borrego, E., Mas, J.L., Martín, J.E., Bolívar, J.P., Vaca, F., Aguado, J.L., 2007. Radioactivity levels in aerosol particles surrounding a large TENORM waste repository after application of preliminary restoration work. Sci. Total Environ. 377 (1), 27–35. https://doi.org/10.1016/j.scitotenv.2007.01.098.

Bouargane, B., et al., 2023a. Portlandite wet-synthesis process from phosphogypsum waste using hydroxide medium: application in both CO_2 capture and brine water salinity reduction. J. Mater. Cycles Waste Manag. https://doi.org/10.1007/s10163-023-01617-8.

Bouargane, B., et al., 2023b. Efective and innovative procedures to use phosphogypsum waste in diferent application domains: review of the environmental, economic challenges and life cycle assessment. J. Mater. Cycles Waste Manag. https://doi.org/10.1007/s10163-023-01617-8.

Bouargane, B., Marrouche, A., El Issiouy, S., Biyoune, M.G., Mabrouk, A., Atbir, A., Bachar, A., Bellajrou, R., Boukbir, L., Bakiz, B., 2019. Recovery of Ca(OH)2, CaCO3, and Na2SO4 from Moroccan phosphogypsum waste. J. Mater. Cycles Waste Manag. 21 (6), 1563–1571.

Bouargane, B., Biyoune, M.G., Mabrouk, A., Bachar, A., Bakiz, B., Ait Ahsaine, H., Mançour Billah, S., Atbir, A., 2020. Experimental Investigation of the Effects of Synthesis Parameters on the Precipitation of Calcium Carbonate and Portlandite from Moroccan Phosphogypsum and Pure Gypsum Using Carbonation Route. Waste and Biomass Valorization 11 (12), 6953–6965.

Bourgier, V., 2008. Influence des ions monohydrogénophosphates et fluorophosphates sur les propriétés des phosphogypses et la réactivité des phosphoplâtres. Thesis report.

Cárdenas-Escudero, C., Morales-Flórez, V., Pérez-López, R., Santos, A., Esquivias, L., 2011. Procedure to use phosphogypsum industrial waste for mineral CO_2 sequestration. J. Hazard. Mater. 196, 431–435. https://doi.org/10.1016/j.jhazmat.2011.09.039.

Christophe, N.N., McCrindle, R., Maree, J., Ngole-Jeme, V., 2023. The behaviour of selected rare-earth elements during the conversion of phosphogypsum to calcium sulphide and residue. J Mate Cycles Waste Manag 25, 1658–1671. https://doi.org/10.1007/s10163-023-.

Contreras, M., Pérez-López, R., Gázquez, M.J., Morales-Flórez, V., Santos, A., Esquivias, L., Bolívar, J.P., 2015. Fractionation and fluxes of metals and radionuclides during the recycling process of phosphogypsum wastes applied to mineral CO_2 sequestration. Waste Manag. 45, 412–419.

Cuesta, E., Barba-Lobo, A., Lozano, R.L., San Miguel, E.G., Mosqueda, F., Bolívar, J.P., 2022. A comparative study of alternative methods for 210Pb determination in

environmental samples. Radiat. Phys. Chem. 191, 109840 https://doi.org/10.1016/j.radphyschem.2021.109840.

El Alaoui-Belghiti, H., Bettach, M., Zdah, I., Ennaciri, Y., Assaoui, J., Zegzouti, A., 2020. Optimization of conditions to convert phosphogypsum into $Ca(OH)_2$ and Na_2SO_4. Moroccan J. Chem. 8 (3), 594–605. https://doi.org/10.48317/IMIST.PRSM/morjchem-v8i3.19328.

El Housse, M., Hadfi, A., Karmal, I., El Ibrahimi, B., Ben-aazza, S., Errami, M., Belattar, M., Mohareb, S., Driouiche, A., 2021a. Valorization of Crocus Sativus L waste extracts as efficient, eco-friendly and economical inhibitors of scaling : Experimental and computational investigations. Mol. Liq. 344, 117718 https://doi.org/10.1016/j.molliq.2021.117718.

El Housse, M., Hadfi, A., Karmal, I., El Ibrahimi, B., Ben-aazza, S., Errami, M., Belattar, M., Mohareb, S., Driouiche, A., 2021b. Experimental investigation and molecular dynamic simulation of Tannic acid as an eco-friendly inhibitor for calcium carbonate scale. Mol. Liq. 340, 117225 https://doi.org/10.1016/j.molliq.2021.117225.

El Housse, M., Hadfi, A., Karmal, I., Tadoumant, T., Ben-aazza, S., Errami, M., Belattar, M., Mohareb, S., Tounsi, A., Driouiche, A., 2021c. Study of scaling problem in the region of tata (Morocco): Analysis of the elemental composition, crystalline phases, and morphologies of scale deposition in water installations. Mol. Liq. 188, 110388 https://doi.org/10.1016/j.apradiso.2022.110388.

El Zrelli, R., Rabaoui, L., Abda, H., Daghbouj, N., Pérez-López, R., Castet, S., Aigouy, T., Bejaoui, N., Courjault-Radé, P., 2019. Characterization of the role of phosphogypsum foam in the transport of metals and radionuclides in the Southern Mediterranean Sea. J. Hazard. Mater. 363, 258–267.

Ennaciri, Y., Bettach, M., 2018. Procedure to convert phosphogypsum waste into valuable products. Mater. Manuf. Process. 33 (16), 1727–1733. https://doi.org/10.1080/10426914.2018.1476763.

Gaudry, A., Zeroual, S., Gaie-Levrel, F., Moskura, M., Boujrhal, F.-Z., El Moursli, R.C., Guessous, A., Mouradi, A., Givernaud, T., Delmas, R., 2007. Heavy metals pollution of the atlantic marine environment by the Moroccan phosphate industry, as observed through their bioaccumulation in Ulva lactuca. Water. Air. Soil Pollut. 178 (1-4), 267–285.

Hammas, I., Horchani-Naifer, K., Férid, M., 2013. Solubility study and valorization of phosphogypsum salt solution. Int. J. Miner. Process. 123, 87–93. https://doi.org/10.1016/j.minpro.2013.05.008.

Harrou, A., Gharibi, E.K., Taha, Y., Fagel, N., El Ouahabi, M., 2020. Phosphogypsum and black steel slag as additives for ecological bentonite-based materials: Microstructure and characterization. Minerals 10 (12), 1–16. https://doi.org/10.3390/min10121067.

Hull, C.D., Burnett, W.C., 1996. Radiochemistry of Florida phosphogypsum. J. Environ. Radioact. 32 (3), 213–238.

Idboufrade, A., Bouargane, B., Ennasraoui, B., Biyoune, M.G., Bachar, A., Bakiz, B., Atbir, A., Mançour-Billah, S., 2022. Phosphogypsum Two-Step Ammonia-Carbonation Resulting in Ammonium Sulfate and Calcium Carbonate Synthesis: Effect of the Molar Ratio OH^-/Ca^{2+} on the Conversion Process. Waste Biomass Valor 13 (3), 1795–1806.

Kacimi, L., Simon-Masseron, A., Ghomari, A., Derriche, Z., 2006. Reduction of clinkerization temperature by using phosphogypsum. J. Hazard. Mater. 137 (1), 129–137. https://doi.org/10.1016/j.jhazmat.2005.12.053.

Khachani, M., El Hamidi, A., Halim, M., Arsalane, S., 2014. Non-isothermal kinetic and thermodynamic studies of the dehydroxylation process of synthetic calcium hydroxide Ca(OH)2. J. Mater. Environ. Sci. 5 (2), 615–624.

Klika, Z., Valášková, M., Bartonová, L., Maierová, P., 2020. Quantitative Evaluation of Crystalline and Amorphous Phases in Clay-Based Cordierite Ceramic. minerals 10 (1122), 1–13. https://doi.org/10.3390/min10121122.

Kuryatnyk, T., Angulski da Luz, C., Ambroise, J., Pera, J., 2008. Valorization of phosphogypsum as hydraulic binder. J. Hazard. Mater. 160 (2–3), 681–687. https://doi.org/10.1016/j.jhazmat.2008.03.014.

Liu, Y., Zhang, Q., Chen, Q., Qi, C., Su, Z., Huang, Z., 2019. Utilisation of water-washing pre-treated phosphogypsum for cemented paste backfill. Minerals 9 (3), 1–20. https://doi.org/10.3390/min9030175.

Lu, S.Q., Lan, P.Q., Wu, S.F., 2016. Preparation of Nano-$CaCO_3$ from Phosphogypsum by Gas-Liquid-Solid Reaction for CO2 Sorption. Ind. Eng. Chem. Res. 55 (38), 10172–10177. https://doi.org/10.1021/acs.iecr.6b02551.

Mas, J.L., Villa, M., Hurtado, S., Garcia-Tenorio, R., 2012. Determination of trace element concentrations and stable lead, uranium and thorium isotope ratios by quadrupole-ICP-MS in NORM and NORM-polluted sample leachates. J. Hazard. Mater. 205, 198–207. https://doi.org/10.1016/j.jhazmat.2011.12.058.

Mattila, H.P., Zevenhoven, R., 2015. Mineral carbonation of phosphogypsum waste for production of useful carbonate and sulfate salts. Frontiers 3, 48. https://doi.org/10.3389/fenrg.2015.00048.

Perez-Moreno, S.M., Gazquez, M.J., Perez-Lopez, R., Vioque, I., Bolívar, J.P., 2018. Assessment of natural radionuclides mobility in a phosphogypsum disposal area. Chemosphere 211, 775–783. https://doi.org/10.1016/j.chemosphere.2018.07.193.

Ramli, N.A.A., Kusin, F.M., Molahid, V.L.M., 2021. Influencing factors of the mineral carbonation process of iron ore mining waste in sequestering atmospheric carbon dioxide. Sustain. 13 (4), 1–17. https://doi.org/10.3390/su13041866.

Rentería-Villalobos, M., Vioque, I., Mantero, J., Manjón, G., 2010. Radiological, chemical and morphological characterizations of phosphate rock and phosphogypsum from phosphoric acid factories in SW Spain. J. Hazard. Mater. 181 (1–3), 193–203. https://doi.org/10.1016/j.jhazmat.2010.04.116.

Rutherford, P.M., Dudas, M.J., Arocena, J.M., 1996. Heterogeneous distribution of radionuclides, barium and strontium in phosphogypsum by-product. Sci. Total Environ. 180 (3), 201–209. https://doi.org/10.1016/0048-9697(95)04939-8.

Silva, L.F.O., Oliveira, M.L.S., Crissien, T.J., Santosh, M., Bolivar, J., Shao, L., Dotto, G.L., Gasparotto, J., Schindler, M., 2022. A review on the environmental impact of phosphogypsum and potential health impacts through the release of nanoparticles. Chemosphere 286, 131513.

Singh, M., Garg, M., 2005. Study on anhydrite plaster from waste phosphogypsum for use in polymerised flooring composition. Constr. Build. Mater. 19 (1), 25–29. https://doi.org/10.1016/j.conbuildmat.2004.04.038.

Tayibi, H., Gascó, C., Navarro, N., López-Delgado, A., Choura, M., Alguacil, F.J., López, F.A., 2011. Radiochemical Characterization of Phosphogypsum for Engineering Use. J. Environ. Prot. (Irvine, Calif) 02 (02), 168–174.

Theo, J., Ding, Z., Martens, W.N., Schuiling, R.D., Duong, L.V., Frost, R.L., 2004. Thermal decomposition of syngenite, $K_2Ca(SO_4)_2.H_2O$. Thermochim. Acta 417 (1), 143–155. https://doi.org/10.1016/j.tca.2003.12.001.

Zairi, M., Rouis, M.J., 1999. Impacts environnementaux du stockage du phosphogypse à Sfax (Tunisie). Bull. des Lab. des ponts chaussées 219, 29–40.

Zdah, I., El Alaoui-Belghiti, H., Cherrat, A., Ennaciri, Y., Brahmi, R., Bettach, M., 2021. Temperature effect on phosphogypsum conversion into potassium fertilizer K_2SO_4 and portlandite. Nanotechnol. 6, 27. https://doi.org/10.1007/s41204-021-00122-3.

Zhu, H., Morris, K., Mueller, W., Field, M., Venkataraman, R., Lamontagne, J., Bronson, F., Berlizov, A., 2009. Validation of true coincidence summing correction in Genie 2000 V3.2. J Radioanal Nucl Chem 282 (1), 205–209.